The IRM Quarterly
Winter 2007, Vol. 16 No. 4



# Electron Holography and Rock Magnetism

Joshua Feinberg[1,2]
Richard Harrison[1]
Takeshi Kasama[1]
Ed Simpson[1]
Rafal Dunin-Borkowski[1]

[1] University of Cambridge
[2] Dep't of Geology and Geophysics, University of Minnesota

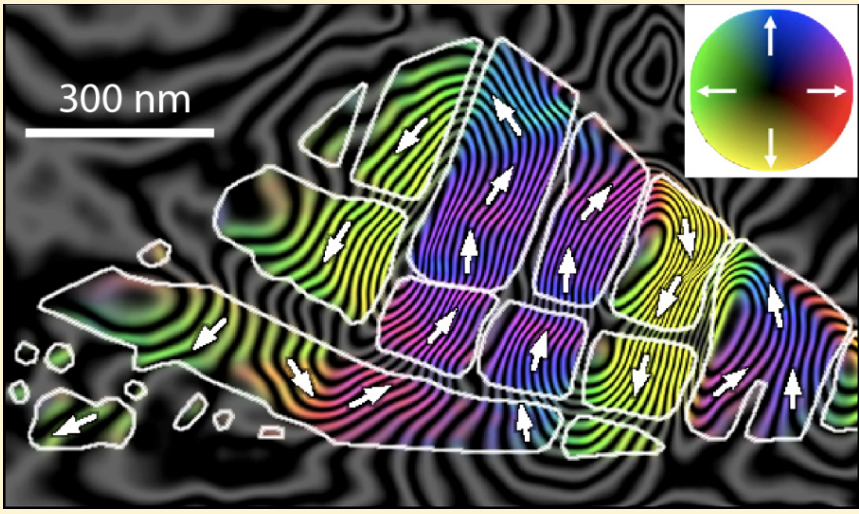


*Figure 1--An example of a fully processed electron hologram showing a cross section through a magnetite/ulvöspinel inclusion exsolved in clinopyroxene. This particular image was collected at 89K (-184˚C). White lines indicate the outline of individual magnetite grains. The magnetization in the plane of the image is indicated using contours, colors, and arrows. The hologram shows the magnetic induction within and between magnetite grains, allowing for the study of non-uniform magnetization within individual grains as well as magnetostatic interactions among populations of grains. Data collected April 2005.*

OVER THE LAST FIVE YEARS a magnetic imaging technique called electron holography has started to be used to image the magnetic flux in geologic materials at nanometer scales (Harrison et al, 2002, 2005; Simpson et al., 2005; Kasama et al., 2006; Feinberg et al., 2006; Harrison et al., 2007). The signature images from these studies are colored, contoured figures showing a sample's magnetic induction and direction (Figure 1). These images are processed versions of data originally collected in a transmission electron microscope (TEM) and contain quantitative information about the magnetization of a sample. The aim of this short article is twofold: to briefly describe the history and procedures intrinsic to electron holography and to encourage others in the rock magnetic community to consider using this technique in their own research by conveying the broad potential the technique has for rock magnetism studies.

## History of Electron Holography

DENNIS GABOR FIRST DESCRIBED electron holography in 1948 as part of a technique proposed to improve the resolution of TEM images (Gabor, 1948). He envisaged an "electron interference microscope" that would capture interference patterns by overlapping two coherent waves of electrons: a "primary" wave that traveled through a region of vacuum, and a "secondary" electron wave that passed through the sample. His interference patterns were characterized by alternating light and dark fringes produced by constructive and destructive interference of the electron waves. When Gabor's interference patterns were re-illuminated using light similar to the "primary" wave, the interference fringes acted as a diffraction grating and produced a virtual image of the original sample. This image reproduction is possible because the interference fringes record information about both the amplitude and the phase of the electron wave leaving the sample.

Even though this discovery would eventually earn Gabor a Nobel Prize in Physics, the development of electron holography lagged until field emission gun (FEG) electron sources became widely available. FEGs provided a reliable source of bright, coherent electrons and they remain a prerequisite for the successful application of the technique. Research groups specializing in electron holography multiplied throughout the 1980s and 1990s and by 1992 over 20 distinct approaches to electron holography had been devised (Cowley, 1992). The brand of holography most useful to rock magnetic studies is "off-axis electron holography" because it

holography, continued on page 6

# Visiting Fellows' Reports

## Bio-mediated formation of magnetite and maghemite particles


### Yohan Guyodo

**LSCE/IPSL, Laboratoire CEA-CNRS-UVSQ**
**Campus du CNRS**
**Gif-sur-Yvette Cedex, France**


MAGNETITE FORMATION IN SOILS and sediments, and its oxidation to maghemite, is a subject of primary importance for various disciplines in earth sciences, which include paleomagnetism, environmental magnetism, and environmental (bio)-geo-chemistry. In loess/paleosols sequences, for instance, deciphering the relative role of biological and inorganic processes in the formation of fine (stable single domain, SSD) or extra-fine (superparamagnetic, SP) particles is an important question in regard to the correct paleoclimatic interpretation of rock magnetic studies. Understanding magnetite/maghemite formation in loess, soils and sediments, is also important for discriminating between possible depositional or pedo/dia-genetic paleomagnetic signals. During my 10-day visit at the IRM, I performed low-temperature magnetic measurements of induced and remanent magnetizations on samples of biogenic magnetite and maghemite formed by bio-mediated alteration of synthetic lepidocrocite (γ-FeOOH), an iron oxyhydroxyde commonly found in the environment.

Biogenic magnetite was prepared via the reduction of lepidocrocite by Shewanella putrefaciens at 30 °C with an initial pH 7.6, in the presence of sodium methanoate (NaHCO2) as electron donor. Anthraquinone-2,6-disulfonate (AQDS), an electron shuttle, was added in the medium in order to enhance the bacterial reduction of ferric oxyhydroxide. In this case, magnetite formation probably proceeds via Fe2+ ions adsorption onto ferric oxyhydroxide surfaces. Maghemite formation was achieved by oxidation of the biogenic magnetite using hydrogen peroxide. Several samples of magnetite and maghemite (corresponding to various experimental conditions) were measured at the IRM, as well as the lepidocrocite used in

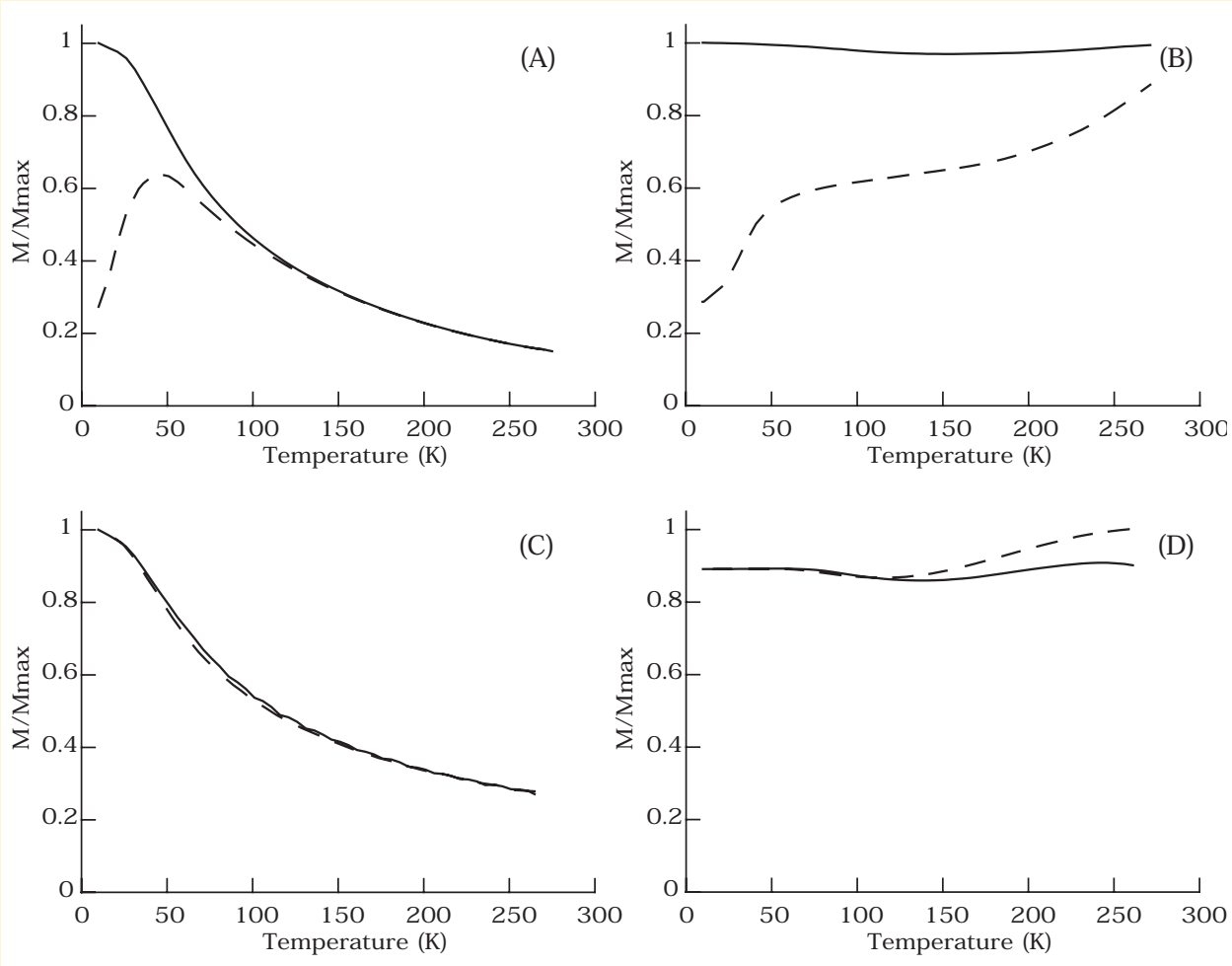


*Induced magnetization measured in a 5 mT field during warming from 10 K, after cooling the sample in zero field (dotted line) or in a 5 mT field (solid line), for lepidocrocite (A) and magnetite (B). Evolution of a room-temperature isothermal remanent magnetization acquired in a 2.5T field, during a cooling (dotted line) and warming (solid line) cycle for lepidocrocite (C) and magnetite (D).*

the reduction experiment. IRM measurements consisted in: (1) Induced magnetizations measured in a 5 mT field during warming of the samples from 10K, after cooling in a zero or 5 mT field (MPMS), (2) magnetic susceptibility as a function of temperature and frequency of the applied field (Lakeshore susceptometer), (3) low-temperature hysteresis loops (micro-VSM), (4) field cooled and zero field cooled remanent magnetization measurements using a 2.5T field (MPMS), (5) high-field (2.5 T) induced magnetization measurements, and (6) cooling-warming cycle of the room temperature isothermal remanent magnetization acquired in 2.5 T (MPMS).

Several interesting results were obtained at the IRM, some of which are illustrated in Figure 1. Concerning lepidocrocite (which is assumed to be antiferromagnetic with a small ferromagnetic-like behavior), the field cooled and zero field cooled induced magnetization curves merge at a temperature around 150 K (Figure 1A). Below this temperature, the difference between the two cures can be explained by the acquisition of a remanent magnetization, acquired during cooling of the sample in the presence of a magnetic field. Therefore, some ferromagnetic-like behavior persists at temperatures above 100 K, even though lepidocrocite has a Néel temperature of about 50 K (Hirt et al., JGR, 107, 10.1029/2001JB000242, 2002). The cooling/warming cycle of the room temperature remanent magnetization (Figure 1C) shows that some remanence can be acquired well above the Néel temperature, and has a variation with temperature probably reflecting that of the saturation magnetization. Further investigations are being conducted in order to better constrain the magnetic behavior of lepidocrocite, in particular using low-temperature high-field VSM measurements (up to 14 T). Concerning the magnetite samples, the main result of my visit is that a large distribution of particle sizes is obtained by reduction of lepidocrocite. As shown in Figure 1B, the field cooled and zero field cooled induced magnetization curves are well separated over the entire temperature interval, which can be interpreted in terms of a large distribution of unblocking temperatures, i.e., particle sizes (interaction between particles will also have to be considered). This is illustrated also in the cooling/warming cycle of the isothermal remanent magnetization (Figure 1D), which indicates that a stable magnetization can be acquired at room temperature by this sample. These measurements indicate that it is possible to obtain magnetite particles able to carry a stable magnetization via extra-cellular bacterial reduction of iron oxyhydroxides by Shewanella putrefaciens. Recently acquired transmission electron microscope images support this observation. I would like to thank the RAC members for letting me use the IRM facilities. I would also like to thank all the people working at the IRM for their warm welcome and their help during my stay.

# A Tale of Two Lakes

## Christoph E. Geiss

**Dept. of Physics, Trinity College, Hartford, CT**

A FEW YEARS AGO Antje Schwalb and colleagues cored Pickerel Lake in northeastern South Dakota and retrieved a quite remarkable susceptibility record. Its rather cyclical variations (Fig. 1a) suggest cyclical environmental changes, most likely periods of extended drought which are leading to an increased deposition of highly magnetic detrital material. To shore up their interpretations they returned to the area, cored nearby Enemy Swim Lake and measured magnetic susceptibility again, only to come up with the rather unimpressive record shown in Fig. 1b. Intrigued by this discrepancy I started analyzing samples from both lakes and found that the two records look a lot more similar and can be cautiously correlated when using remanence measurements rather than in-field measurements (ARM records shown in Fig. 2).

With both lakes possibly recording similar regional climate signals, I came to the IRM to further perform some low-temperature analyses to constrain the magnetic mineralogy and measure hysteresis loops to quantify the presence of para- and diamagnetic minerals that might hold the key to the observed differences between the magnetic susceptibility and remanence records.

After several MPMS analyses (Fig. 3) and Curie-temperature measurements (not shown) the magnetic mineralogy still remains somewhat elusive. Thermal demagnetization of a low-temperature remanence acquired through field cooling shows a plateau below 20 - 30 K indicative of either siderite (Housen et al., 1996) or iron sulfides (Rochette et al., 1990) and a weak hint of a Verwey transition. Curie-temperature measurement performed at Trinity College remained inconclusive due to the weak magnetic signal of the sample. To make things more ambiguous, no distinct smell of sulfur was detected during heating, nor was siderite identified during X-ray diffraction analyses. Alternating field demagnetization curves of IRM acquired in a field of 1.5T at room temperature (Fig. 4) identify a magnetic phase with a mean destructive field between 25 - 35 mT. In addition more than 90% of the IRM signal is demagnetized by alternating fields between 100 mT and 110 mT indicating the presence of a magnetically soft ferrimagnetic phase, most likely oxidized magnetite.

The differences between magnetic susceptibility and magnetic remanence can be caused by changes in mineralogy or grain size. To estimate the importance of dia- or paramagnetic minerals on the magnetic signal we measured hysteresis loops for both lakes and calculated the paramagnetic susceptibility from the high-field slope of the loops. As it becomes obvious from Fig. 1 (solid symbols) variations in para- or diamagnetic minerals cannot explain the observed differences between susceptibility and remanence. In hindsight this result might have been

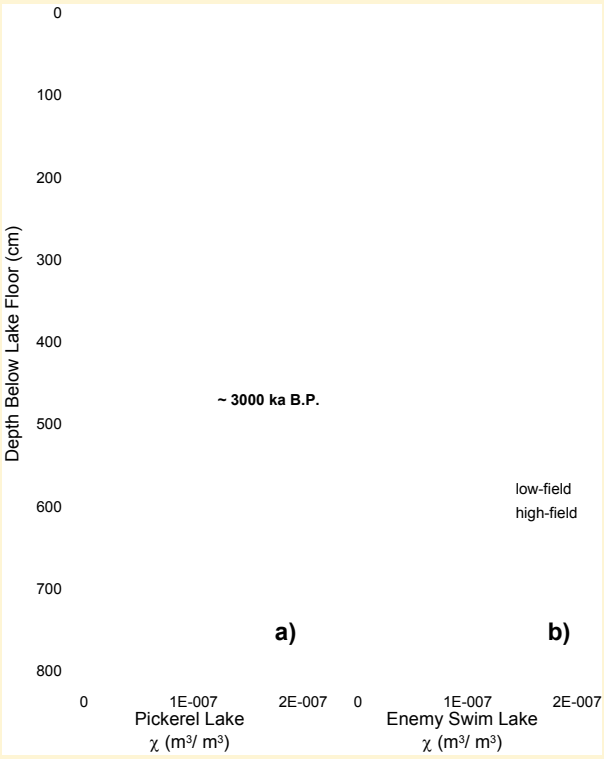


*Figure 1--Susceptibility records for a) Pickerel lake and b) Enemy Swim Lake. Influence of high-field susceptibility on the magnetic susceptibility record of both lakes is generally low and does not account for the discrepancy between susceptibility and remanence records.*

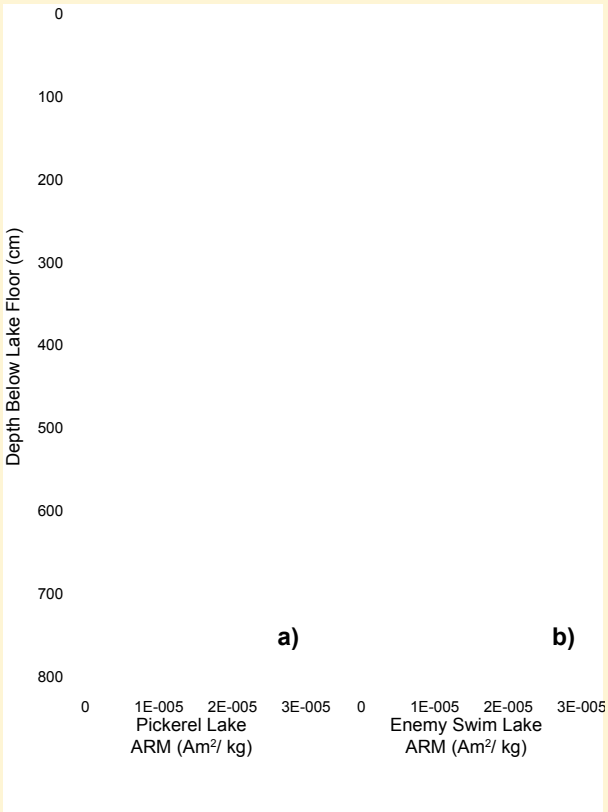


*Figure 2--ARM records of a) Pickerel Lake and b) Enemy Swim Lake.*

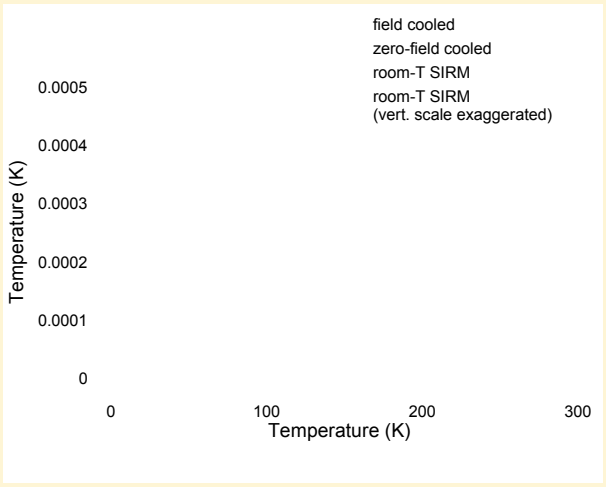


*Figure 3--Low-temperature measurements for Pickerel Lake, 231 cm.*

expected given the vast differences in susceptibility between para- and ferrimagnetic minerals (e.g., Hunt et al., 1995). Any major changes in para- or diamagnetic minerals would have diluted the ferrimagnetic component thus affecting both susceptibility and remanence.

Plotting the hysteresis results in a Day plot (Day et al., 1977) shows that samples from Enemy Swim Lake tend to have coarser bulk magnetic grain sizes than samples from Pickerel Lake (Fig. 5). To assess the presence of ultra-fine superparamagnetic (SP) minerals we calculated the ratio IRM/$\chi$ which is shown for both lakes in Fig. 6. Combining the results shown in Figs 5 and 6 reveals a bimodal grain size distribution for samples from Enemy Swim lake which appear to contain a mixture of coarse multi-domain (MD) and SP particles, indicative of pervasive dissolution and later recrystallization of ferrimagnetic minerals (e.g., Tarduno, 1995).

Both lakes are located in very similar parent material, within two miles of each other and should record similar climatic conditions. However, the water chemistry of both lakes differs as Pickerel Lake is a closed basin while Enemy Swim Lake has several inflows as well as an outflow stream to the southwest. It appears that both records are more similar below 5 m depth, which corresponds to an approximate sediment age or 3 - 3.5 ka B.P. (Schwalb, pers. comm.). Diatom analyses from Moon Lake in nearby North Dakota (Laird et al., 1996) reveal drier climatic conditions between 2.5 - 7 ka B.P. Generally drier conditions during this time period may have resulted in a lowering of lake levels at Enemy Swim Lake below its present outflow, making the two lakes more similar.

Changes in remanence parameters (including ARM as shown in Fig.2) mainly reflect changes in the concentration of remanence-carrying ferrimagnetic minerals, are less sensitive to changes in magnetic grain size, and are furthermore completely blind to the presence of SP ferrimagnetic particles. To determine the exact environmental processes that govern the observed rock-magnetic changes will require additional geochemical measurements that are

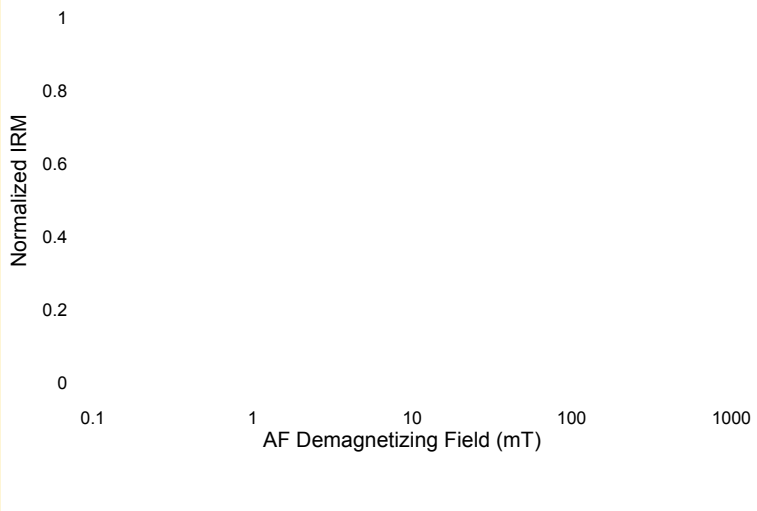


*Figure 4--IRM demagnetization curves for eight samples from Pickerel Lake.*

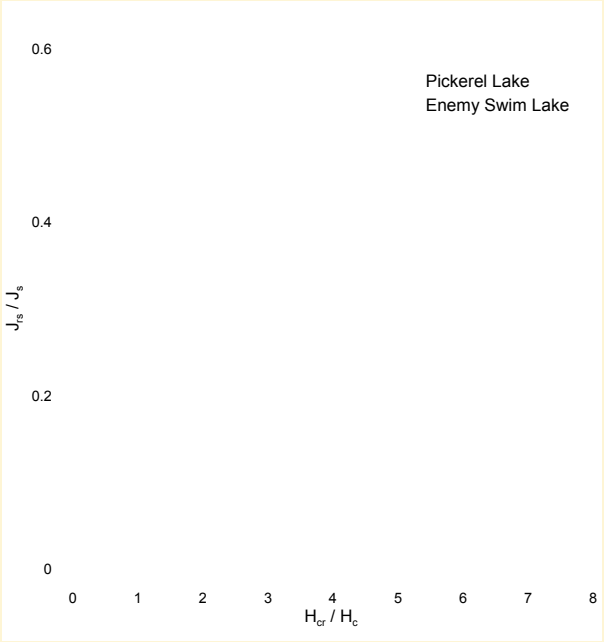


*Figure 5--Hysteresis data for samples from Pickerel Lake (closed symbols) and enemy Swim lake (open symbols).*

currently underway, but the magnetic records of Pickerel and Enemy Swim Lakes may well hold the key to a high resolution climate reconstruction.

## References


Day, R., Fuller, M., and Schmidt, V. A. (1977). Hysteresis properties of titanomagnetites: Grain-size and compositional dependence. Physics of the Earth and Planetary Interiors 13, 260-267.

Housen, B. A., Banerjee, S. K., and Moskowitz, B. M. (1996). Low-temperature magnetic properties of siderite and magnetite in marine sediments. Geophysical Research Letters 23, 2843-2846.

Hunt, C. P., Moskowitz, B. M., and Banerjee, S. K. (1995). Magnetic properties of rocks and minerals. In "Rock Physics and Phase Relations. A Handbook of Physical Constants." pp. 189-204. AGU Reference Shelf.

Laird, K. R., Fritz, S. C., Grimm, E. C., and Mueller, P. G. (1996). Century-Scale Paleoclimatic Reconstruction from Moon Lake, a Closed-Basin Lake in the Northern Great Plains. Limnology and Oceanography 41, 890-902.

Rochette, P., Fillion, G., Mattei, J. L., and Dekkers, M. J. (1990). Magnetic transition at 30-34 Kelvin in pyrrhotite: insight into a widespread occurrence of this mineral in rocks. Earth & Planetary Science Letters 98, 319-328.

Tarduno, J. A. (1995). Superparamagnetism and reduction diagenesis in pelagic sediments: Enhancement or depletion? Geophysical Research Letters 22, 1337-1340.


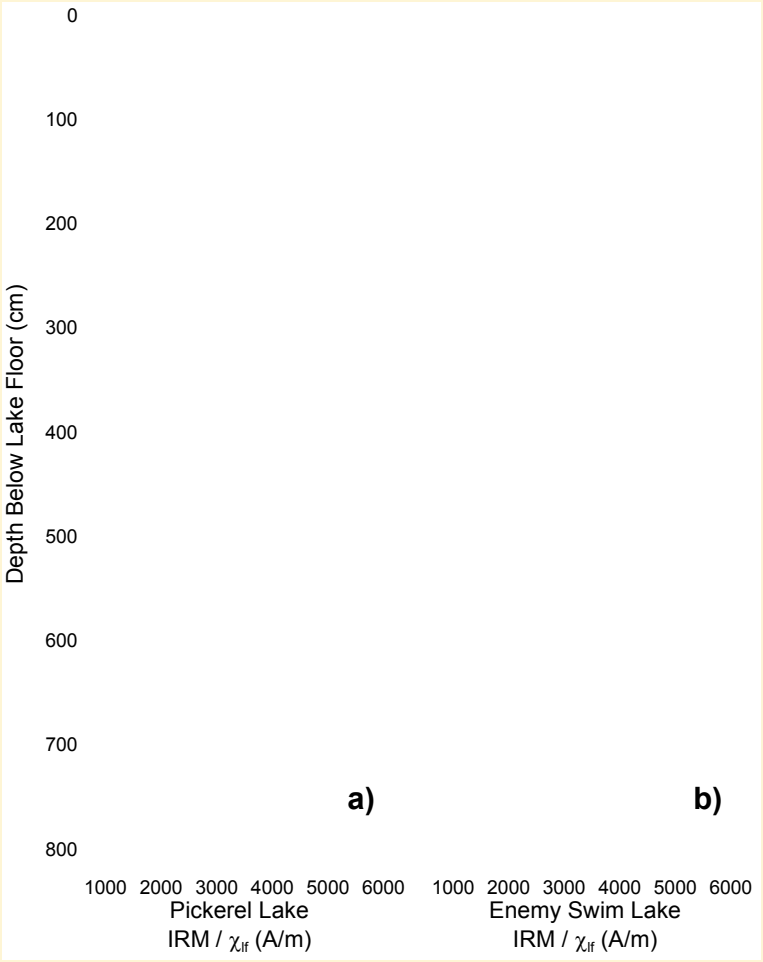


*Figure 6--Changes in IRM / χ for a) Pickerel lake and b) Enemy Swim Lake.*

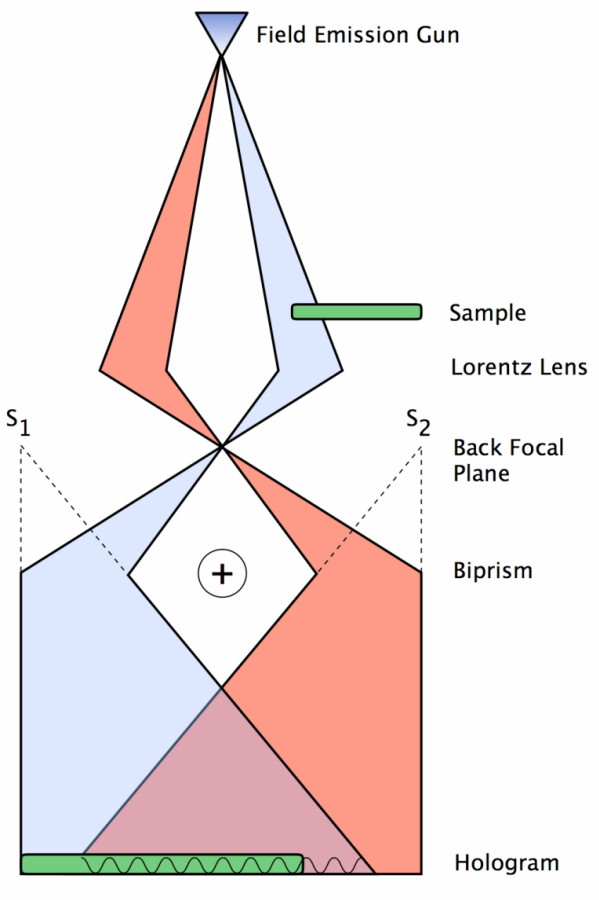


*Figure 2--Schematic illustration of the TEM setup used in off-axis electron holography. The sample occupies approximately half the field of view. Critical components are the field emission gun, which provides a source of coherent electron illumination, and the positively charged electron biprism wire, which acts to overlap the sample and (vacuum) reference waves. The Lorentz lens allows imaging of magnetic minerals in a close-to-field-free environment (<0.5 mT). (Adapted from Harrison et al., 2007)*

**holography, from page 1**

focuses on isolating the phase shift induced by a magnetic material rather than on producing virtual images. A detailed explanation of the theory of off-axis electron holography requires more space than is available here and readers are urged to explore the excellent reviews of the technique by Dunin-Borkowski & McCartney (2002) and Dunin-Borkowski et al., (2004).

## Experimental Design

A SCHEMATIC FIGURE of the experimental setup for an off-axis electron holography study of magnetic materials is shown in Figure 2. In addition to the FEG, two important hardware modifications are required: the installation of a Lorentz lens and an electrostatic biprism. In conventional TEM practice, the current in an electromagnetic objective lens is used to produce high magnification images of a sample. However, the objective lens is unsuitable for imaging during off-axis electron holography of magnetic materials because it produces a large magnetic field that can alter the magnetic structure in a mineral sample. Instead, a Lorentz lens is installed below the conventional objective lens to allow for work at high magnification while keeping the sample in a relatively field-free environment (<0.5 mT). The objective lens is turned off, or is turned on temporarily to impart fields of up to 2 T to the sample. An electrostatic biprism, typically a gold-coated quartz wire (or platinum wire), is installed in one of the selected-area apertures of the TEM. When a voltage is applied to the biprism (between 50-250 V), portions of the electron beam are deflected so that they overlap (Figure 2). This overlap produces an interference pattern (a hologram), which appears as a typical bright-field TEM image overlain by interference fringes. The broader interference fringes are called Fresnel fringes and are due to diffraction around the edges of the biprism wire, while the fine-scale interference fringes contain information about both the amplitude and the phase shift experienced by the electrons as they pass though the mineral sample. The magnitude of the phase shift is due to factors such as the sample's thickness, its mean inner potential (a measure of a material's ability to slow passing electrons), and its magnetization. Because rock magnetists are primarily interested in the magnetically induced phase shift, the contributions from the sample's thickness and mean inner potential must be removed. Thus, off-line processing is required to extract the magnetic data from a raw holographic image. This processing is made significantly easier if the original holograms are collected on a charged-coupled device (CCD) camera, rather than on photographic film.

*"The aim of this short article is twofold: to briefly describe the history and procedures intrinsic to electron holography and to encourage others in the rock magnetic community to consider using this technique in their own research."*

## Processing the Holograms

AT THE UNIVERSITY OF CAMBRIDGE, holograms are digitally processed using a series of routines that run in a software environment named Semper. An example of an unprocessed hologram is shown in Figure 3a. A magnetically induced phase shift can be seen in the fine-scale interference fringes as they are displaced while passing over a maghemite inclusion exsolved in hematite (inset in Figure 3a). An unprocessed hologram from a region of vacuum is shown for comparison in Figure 3b. A Fourier transform of the hologram in 3a is shown in Figure 3c, comprising a central peak, two side bands, and a diagonal streak due to the Fresnel fringes. In order to isolate the phase shift information and remove the portions of the image due to direct transmittance and Fresnel fringes, a "complex image wave" is produced through an inverse Fourier transform of an isolated side

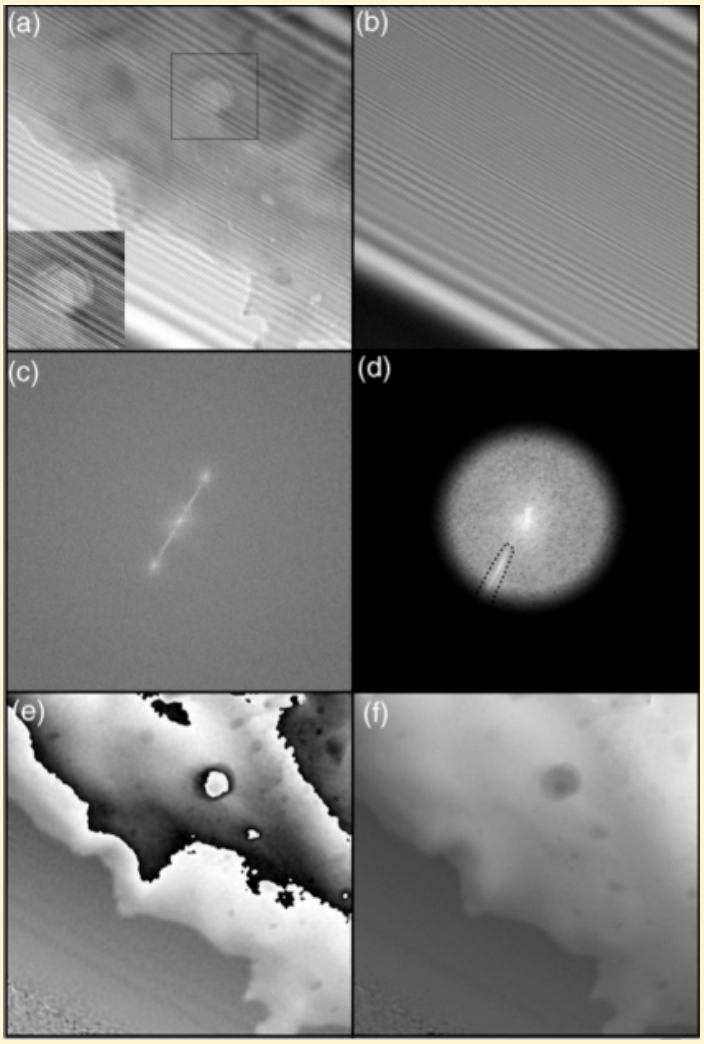


*Figure 3--The sequence of image processing steps required to convert an electron hologram into a phase shift image. (a) Original electron hologram of the region of interest (in this instance a maghemite-bearing hematite). Broad Fresnel fringes caused by diffraction around the edge of the biprism wire are visible in the upper right and lower left. The inset is a magnified image of the outlined region, showing the change in position of the fine-scale holographic fringes as they pass through a maghemite inclusion. (b) A reference hologram recorded over a region of vacuum. (c) Fourier transform of the electron hologram shown in (a), comprising a central peak, two side bands, and a diagonal streak due to the Fresnel fringes. (d) A mask is applied to the Fourier transform in (c) in order to isolate one side band. The Fresnel streak is removed by assigning a value of zero to pixels falling inside the region shown by the dashed line. (e) Inverse Fourier transform of (d) yields the complex image wave, which in turn yields a modulo 2π image of the holographic phase shift. (f) Automated phase unwrapping algorithms are used to remove the 2π phase discontinuities from (e) to yield the final phase shift image. (Adapted from Harrison et al., 2007)*

band (Figure 3e). The sample's complex image wave is divided by that of the vacuum hologram in order to remove phase shifts caused by heterogeneities in the charge and thickness of the biprism wire. Because the total range of phase shifts across the final complex image wave is greater than 2π, phase shift discontinuities form across the image. These phase discontinuities can be removed (or "unwrapped") using automated image processing routines to yield the final phase shift image (Figure 3f).

The next step is to remove the mean inner potential contribution to the phase shift. If a sample's magnetization can be perfectly reversed (e.g., by saturation in two opposite directions), then the magnetic contribution in the resulting phase shift images will be opposite in sign. Such images can be straightforwardly gathered by using the magnetic field generated by the objective lens to saturate the sample in opposite directions. By adding two reversely magnetized images, the magnetic contribution to the phase shift cancels out, leaving behind twice the mean inner potential contribution. In practice, some samples do not reverse precisely the same way, and the reversal measurements must be repeated multiple times so that nonsystematic differences between reversed images average out. Once the mean inner potential contribution has been determined in this way, it can be removed from the final phase shift images, leaving behind an image of only the magnetically induced phase shift.

Visualizing the resulting phase shift image can be accomplished using contours, colors, and arrows. Contours can be produced by plotting the cosine of the phase shift. The spacing of the contours can be adjusted by multiplying the phase shift by a constant (an "amplification factor") before taking its cosine. For example, the simulated contour plots shown in Figure 4g-i were produced using an amplification factor of four. By calculating the vertical and horizontal derivatives of the phase shift, the direction and magnitude of the projected in-plane magnetic induction can be represented by the hue and intensity of a color. Alternatively, this vector field can be portrayed using arrows.

*"[E]lectron holography offer[s] us the opportunity to visualize otherwise invisible magnetic structures at unprecedented spatial resolution (~5 nm)."*

One of the strengths of the off-axis electron holography technique is that lines of magnetic flux are imaged quantitatively both within and between magnetic grains. This style of visualization allows researchers to study non-uniform magnetizations within grains as well as magnetostatic interactions among populations of grains. However, like any technique, off-axis electron holography has its limitations. The magnetization of a sample must be relatively strong (>50 kA m-1) in order to discern the magnetic component of the phase shift at a scale of ~10 nm. If such high resolution is not required then it is possible to study more weakly magnetized materials such as hematite or goethite. Additionally, holograms show only the in-plane magnetization of a sample. One highly anticipated development in off-

axis electron holography is the development of vector field tomography, which may allow a three-dimensional image of the magnetic induction throughout a sample to be produced.

## Additional Advantages

THERE ARE NUMEROUS additional advantages to using electron holography in rock magnetic studies. Recent TEM models allow users to adjust the environment inside the TEM column, so that the conditions under which a mineral acquires its natural remanent magnetization can be reproduced. A sample's temperature can be varied; mixtures of oxidizing or reducing gases can be introduced; and the ambient magnetic field can be carefully controlled. The composition of magnetic minerals can be precisely determined using energy dispersive spectroscopy (EDS) or electron energy loss spectroscopy (EELS). A mineral's orientation and crystal structure can be determined using standard selected-area electron diffraction (SAED) or the more advanced technique of convergent beam electron diffraction (CBED). The distribution of grain shapes and sizes in a TEM specimen can be measured in three-dimensions using electron tomography (Figure 5). There is also the potential to use alternative magnetic imaging modes such as the Frsenel mode of Lorentz microscopy.

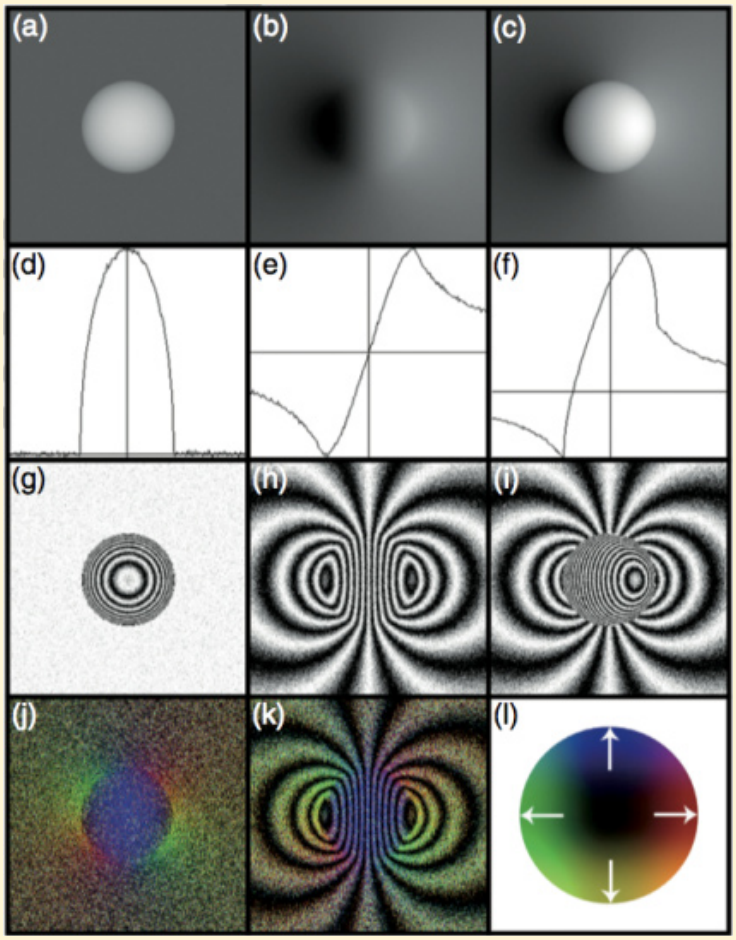


*Figure 4--Simulation of the holographic phase shift associated with a 200 nm diameter spherical particle of magnetite. The particle is uniformly magnetized in the vertical direction. The mean inner potential contribution to the phase shift is shown in (a), the magnetic contribution in (b), and the sum of the two is shown in (c). (d-f) Profiles of (a-c), taken horizontally through the center of the particle (normal to the magnetization direction). (g-i) Cosine of 4 times the phase shift shown in (a-c). (j) Color map derived from the slope (gradient) of the magnetic contribution to the phase shift (b). The hue and intensity of the color indicates the direction and magnitude of the integrated in-plane component of magnetic induction, according to the color wheel show in (l). The color can be combined with the contour map (k). (Adapted from Harrison et al., 2007.)*

The number of laboratories around the world capable of conducting electron holography studies is increasing. Established laboratories with interests in rock magnetism already exist at the University of Cambridge and Arizona State University. New facilities are being built at the University of Alberta and the Technical University of Denmark and should be operational by late summer of 2007.

Magnetic imaging is advancing quickly. Techniques such as electron holography offer us the opportunity to visualize otherwise invisible magnetic structures at unprecedented spatial resolution (~5 nm). Images at this scale are introducing us to never-before-seen magnetic structures that challenge our existing models of fundamental magnetic phenomena such as exchange coupling and magnetostatic interactions. But as Freddie Mercury once said, "If you see it, darling, then it's there." The magnetic structures seen using electron holography and other imaging techniques such as magnetic force microscopy are ushering in an exciting era, where new micromagnetic models are needed to help understand these latest high-resolution observations.

*"The number of laboratories around the world capable of conducting electron holography studies is increasing. Established laboratories with interests in rock magnetism already exist at the University of Cambridge and Arizona State University. New facilities are being built at the University of Alberta and the Technical University of Denmark and should be operational by late summer of 2007."*

## Bibliography

Cowley, J.M. Twenty forms of electron holography, Ultramicroscopy, 41, 335-348, 1992.

Dunin-Borkowski, R.E., M.R. McCartney, D.J. Smith, Electron holography of nanostructured materials. *In* Nalwa, H.S., ed., Encyclopedia of nanoscience and nanotechnology, Vol. 3. Stevenson Ranch, CA: American Scientific Publishers. p. 41-100. 2004.

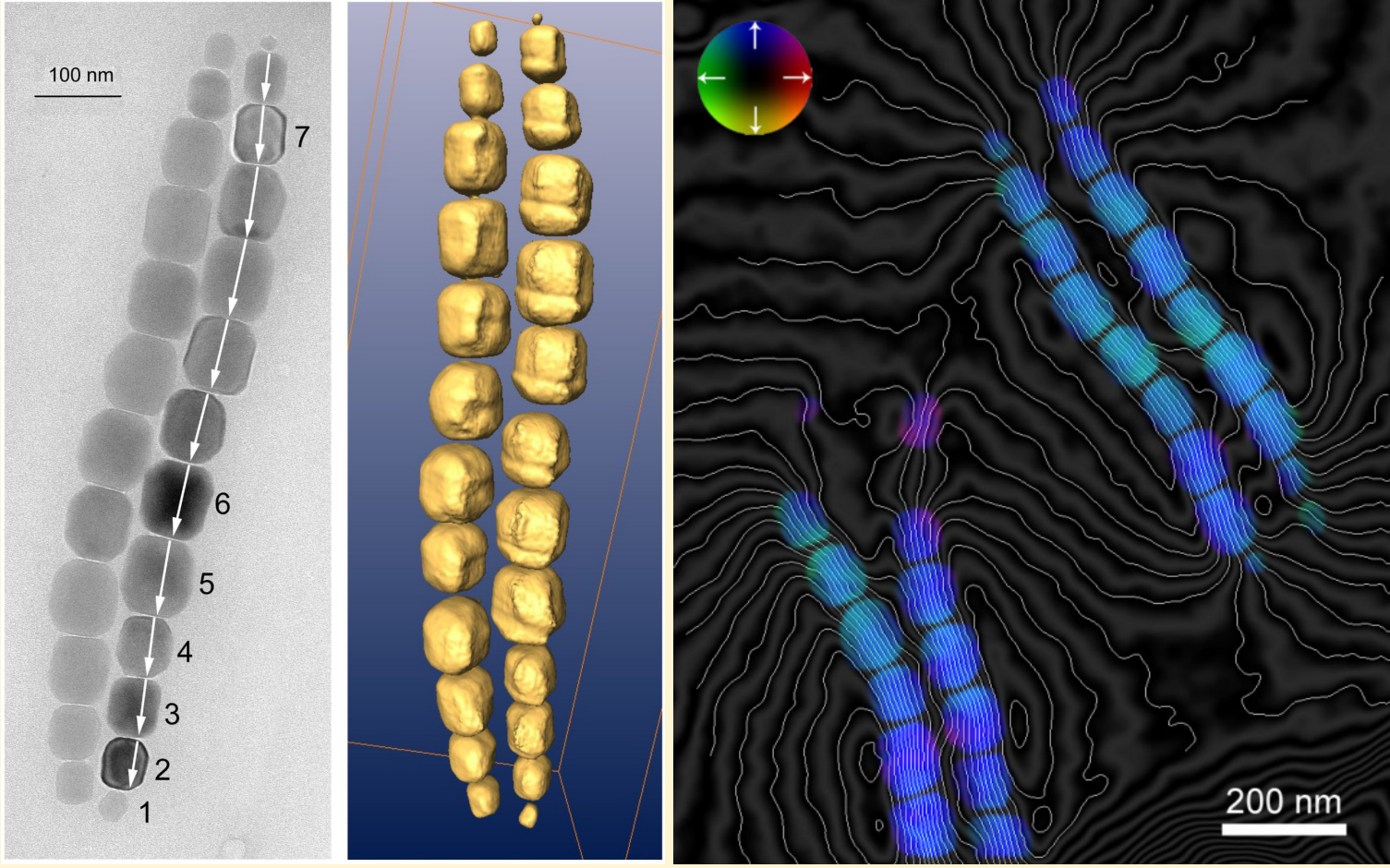


*Figure 5--TEM study of magnetotactic bacteria. The image on the left shows a bright-field TEM image of magnetotactic bacteria, where white arrows indicate the approximate orientation of the magnetite [111] axis in each magnetosome. The middle image shows a three-dimensional reconstruction of the same magnetosomes using electron tomography. The image on the right is an electron holography image of bacteria in the same sample. The direction of in-plane magnetization is given by the contours and colors. (See the color wheel inset.) Magnetic interactions between magnetosomes force the final magnetization direction to be parallel to the elongation of the chain. (Adapted from Harrison et al., 2007.)*

Dunin-Borkowski, R.E., T. Kasama, A. Wei, S. Tripp, M.J. Hÿtch, E. Snoeck, R.J. Harrison, and A. Putnis, Off-axis electron holography of magnetic nanowires and chains, rings, and planar arrays of magnetic nanoparticles, Microscopy Research and Technique, 64, 390-402, 2004.

Feinberg, J.M., R.J. Harrison, T. Kasama, R.E. Dunin-Borkowski, G.R. Scott, P.R. Renne, Effects of internal mineral structures on the magnetic remanence of silicate-hosted titanomagnetite inclusions: An electron holography study, Journal of Geophysical Research, 111, B12S15, doi:10.1029/2006JB004498. 2006.

Gabor, D. A New Microscopic Principle, Nature, 161, 777-778, 1948.

Harrison, R.J., R.E. Dunin-Borkowski, and A. Putnis, Direct imaging of nanoscale magnetic interactions in minerals, Proceedings of the National Academy of Sciences of the United States of America, 99, 16556-16561, 2002.

Harrison, R.J., T. Kasama, T. A. White, E. T. Simpson, and R. E. Dunin-Borkowski, Origin of self-reversed thermoremanent magnetization, Physical Review Letters, 95, 268501, 2005.

Harrison, R.J., R.E. Dunin-Borkowski, T. Kasama, E.T. Simpson, and J.M. Feinberg, Magnetic properties of rocks and minerals, Chapter to be published in the "Treatise on Geophysics", edited by G Schubert, Elsevier, ISBN 0444519289, 2007.

Kasama, T., M. Posfai, R.K.K. Chong, A.P. Finlayson, P.R. Buseck, R.B. Frankel, and R.E. Dunin-Borkowski, Magnetic properties, microstructure, composition, and morphology of greigite nanocrystals in magnetotactic bacteria from electron holography and tomography., American Mineralogist, 91, 1216-1229, 2006.

Simpson, E.T., T. Kasama, M. Pósfai, P.R. Buseck, R.J. Harrison, and R.E. Dunin-Borkowski, Magnetic induction mapping of magnetite chains in magnetotactic bacteria at room temperature and close to the Verwey transition using electron holography, Journal of Physics: Conference Series 17 108-121, 2005.

## New Faculty Member at IRM

Josh Feinberg will be starting as an assistant professor of Geophysics this fall at the University of Minnesota. We, here at IRM, are excited to have Josh join us. Josh's arrival is exciting on two fronts: We are thrilled to begin exploring unfamiliar avenues of research under Josh's lead as a new colleague; and we are equally thrilled to welcome Josh into the IRM fold as an old friend. We are sure that *Quarterly* readers will join us in welcoming and congratulating Josh.

# Current Articles

A list of current research articles dealing with various topics in the physics and chemistry of magnetism is a regular feature of the IRM Quarterly. Articles published in familiar geology and geophysics journals are included; special emphasis is given to current articles from physics, chemistry, and materials-science journals. Most abstracts are taken from INSPEC (© Institution of Electrical Engineers), Geophysical Abstracts in Press (© American Geophysical Union), and The Earth and Planetary Express (© Elsevier Science Publishers, B.V.), after which they are subjected to Procrustean culling for this newsletter. An extensive reference list of articles (primarily about rock magnetism, the physics and chemistry of magnetism, and some paleomagnetism) is continually updated at the IRM. This list, with more than 10,000 references, is available free of charge. Your contributions both to the list and to the Abstracts section of the IRM Quarterly are always welcome.

## Alteration and Remagnetization

Frank, U., N.R. Nowaczyk, and J.F.W. Negendank, Palaeomagnetism of greigite bearing sediments from the Dead Sea, Israel, Geophysical Journal International, 168 (3), 904-920, 2007.

Park, Y.H., S.J. Doh, and D. Suk, The Early Tertiary chemical remagnetization in the Bakjisan Syncline, Korea: Its geotectonic implications, Physics of the Earth and Planetary Interiors, 160 (3-4), 269-284, 2007.

## Anisotropy

Kapicka, A., F. Hrouda, E. Petrovsky, and J. Polacek, Effect of plastic deformation in laboratory conditions on magnetic anisotropy of sedimentary rocks, High Pressure Research, 26 (4), 549-553, 2006.

## Biogeomagnetism

Carlut, J., H. Horen, and D. Janots, Impact of micro-organisms activity on the natural remanent magnetization of the young oceanic crust, Earth and Planetary Science Letters, 253 (3-4), 497-506, 2007.

Ehrhardt, C.J., R.M. Haymon, M.G. Lamontagne, and P.A. Holden, Evidence for hydrothermal Archaea within the basaltic flanks of the East Pacific Rise, Environmental Microbiology, 9 (4), 900-912, 2007.

Houghton, J.L., W.E. Seyfried, A.B. Banta, and A.L. Reysenbach, Continuous enrichment culturing of thermophiles under sulfate and nitrate-reducing conditions and at deep-sea hydrostatic pressures, Extremophiles, 11 (2), 371-382, 2007.

Jones, B., and R.W. Renaut, Selective mineralization of microbes in Fe-rich precipitates (jarosite, hydrous ferric oxides) from acid hot springs in the Waiotapu geothermal area, North Island, New Zealand, Sedimentary Geology, 194 (1-2), 77-98, 2007.

Lang, C., D. Schuler, and D. Faivre, Synthesis of magnetite nanoparticles for bio- and nanotechnology: Genetic engineering and biomimetics of bacterial magnetosomes, Macromolecular Bioscience, 7 (2), 144-151, 2007.

Minyard, M.L., and W.D. Burgos, Hydrologic flow controls on biologic iron(III) reduction in natural sediments, Environmental Science & Technology, 41 (4), 1218-1224, 2007.

Thalau, P., T. Ritz, H. Burda, R.E. Wegner, and R. Wiltschko, The magnetic compass mechanisms of birds and rodents are based on different physical principles, Journal of the Royal Society Interface, 3 (9), 583-587, 2006.

Zavarzina, D.G., T.G. Sokolova, T.P. Tourova, N.A. Chernyh, N.A. Kostrikina, and E.A. Bonch-Osmolovskaya, Thermincola ferriacetica sp nov., a new anaerobic, thermophilic, facultatively chemolithoautotrophic bacterium capable of dissimilatory Fe(III) reduction, Extremophiles, 11 (1), 1-7, 2007.

## Environmental Magnetism

Bidegain, J.C., A.J. van Velzen, and Y. Rico, The Brunhes/Matuyama boundary and magnetic parameters related to climatic changes in Quaternary sediments of Argentina, Journal of South American Earth Sciences, 23 (1), 17-29, 2007.

Francis, A.A., Magnetic characteristics of iron-containing glass originated from the mixture of various wastes, Ceramics International, 33 (2), 163-168, 2007.

Frank, U., N.R. Nowaczyk, and J.F.W. Negendank, Rock magnetism of greigite bearing sediments from the Dead Sea, Israel, Geophysical Journal International, 168 (3), 921-934, 2007.

Li, Y.X., Z.C. Yu, and K.P. Kodama, Sensitive moisture response to Holocene millennial-scale climate variations in the Mid-Atlantic region, USA, Holocene, 17 (1), 3-8, 2007.

Shi, R.P., and M.T. Cioppa, Magnetic survey of topsoils in Windsor-Essex County, Canada, Journal of Applied Geophysics, 60 (3-4), 201-212, 2006.

Stucki, J.W., K. Lee, B.A. Goodman, and J.E. Kostka, Effects of in situ biostimulation on iron mineral speciation in a subsurface soil, Geochimica Et Cosmochimica Acta, 71 (4), 835-843, 2007.

Walden, J., E. Wadsworth, W.E.N. Austin, C. Peters, J.D. Scourse, and I.R. Hall, Compositional variability of ice-rafted debris in Heinrich layers 1 and 2 on the northwest European continental slope identified by environmental magnetic analyses, Journal of Quaternary Science, 22 (2), 163-172, 2007.

Xia, D.S., X. Chun, J. Bloemendal, R.C. Chiverrell, and F. Chen, Use of magnetic signatures to correlate tephra layers in Holocene loessial soil profiles from a small region, SE Iceland, Environmental Geology, 51 (8), 1425-1437, 2007.

Zhang, C.X., B.C. Huang, Z.Y. Li, and H. Liu, Magnetic properties of high-road-side pine tree leaves in Beijing and their environmental significance, Chinese Science Bulletin, 51 (24), 3041-3052, 2006.

## Extraterrestrial Magnetism

Amils, R., E. Gonzalez-Toril, D. Fernandez-Remolar, F. Gomez, A. Aguilera, N. Rodriguez, M. Malki, A. Garcia-Moyano, A.G. Fairen, V. de la Fuente, and J.L. Sanz, Extreme environments as mars terrestrial analogs: The Rio Tinto case, Planetary and Space Science, 55 (3), 370-381, 2007.

Chevrier, V., and P.E. Mathe, Mineralogy and evolution of the surface of Mars: A review, Planetary and Space Science, 55 (3), 289-314, 2007.

Gilder, S.A., M. Le Goff, and J.C. Chervin, Static stress demagnetization of single and multidomain magnetite with implications for meteorite impacts, High Pressure Research, 26 (4), 539-547, 2006.

Klingelhofer, G., R.V. Morris, P.A. De Souza, D. Rodionov, and C. Schroder, Two earth years of Mossbauer studies of the surface of Mars with MIMOS II, Hyperfine Interactions, 170 (1-3), 169-177, 2006.

Langlais, B., and M. Purucker, A polar magnetic paleopole associated with Apollinaris Patera, Mars, Planetary and Space Science, 55 (3), 270-279, 2007.

Louzada, K.L., S.T. Stewart, and B.P. Weiss, Effect of shock on the magnetic properties of pyrrhotite, the Martian crust, and meteorites, Geophysical Research Letters, 34 (5), 2007.

Quesnel, Y., B. Langlais, and C. Sotin, Local inversion of magnetic anomalies: Implication for Mars' crustal evolution,

Planetary and Space Science, 55 (3), 258-269, 2007.
Shahnas, H., and J. Arkani-Hamed, Viscous and impact demagnetization of Martian crust, Journal of Geophysical Research-Planets, 112 (E2), 2007.

## Magnetic Field Records and Paleointensity Methods

Courtillot, V., Y. Gallet, J.L. Le Mouel, F. Fluteau, and A. Genevey, Are there connections between the Earth's magnetic field and climate?, Earth and Planetary Science Letters, 253 (3-4), 328-339, 2007.
Dumberry, M., and C.C. Finlay, Eastward and westward drift of the Earth's magnetic field for the last three millennia, Earth and Planetary Science Letters, 254 (1-2), 146-157, 2007.
Dunlop, D.J., Palaeomagnetism - A more ancient shield, Nature, 446 (7136), 623, 2007.
Herrero-Bervera, E., E.J. Browne, J.P. Valet, B.S. Singer, and B.R. Jicha, Cryptochron C2r.2r-1 recorded 2.51 Ma in the Koolau Volcano at Halawa, Oahu, Hawaii, USA: Paleomagnetic and Ar-40/Ar-39 evidence, Earth and Planetary Science Letters, 254 (3-4), 256-271, 2007.
Kristjansson, L., and G. Jonsson, Paleomagnetism and magnetic anomalies in Iceland, Journal of Geodynamics, 43 (1), 30-54, 2007.
Leonhardt, R., and K. Fabian, Paleomagnetic reconstruction of the global geomagnetic field evolution during the Matuyama/Brunhes transition: Iterative Bayesian inversion and independent verification, Earth and Planetary Science Letters, 253 (1-2), 172-195, 2007.
Tarduno, J.A., R.D. Cottrell, M.K. Watkeys, and D. Bauch, Geomagnetic field strength 3.2 billion years ago recorded by single silicate crystals, Nature, 446 (7136), 657-660, 2007.

## Magnetic Microscopy and Spectroscopy

Chen, K.F., S.C. Lo, L. Chang, R. Egerton, J.J. Kai, J.J. Lin, and F.R. Chen, Valence state map of iron oxide thin film obtained from electron spectroscopy imaging series, Micron, 38 (4), 354-361, 2007.
Gaviria, J.P., A. Bohe, A. Pasquevich, and D.M. Pasquevich, Hematite to magnetite reduction monitored by Mossbauer spectroscopy and X-ray diffraction, Physica B-Condensed Matter, 389 (1), 198-201, 2007.
Harrison, R.J., Neutron diffraction of magnetic materials, in Neutron Scattering in Earth Sciences, pp. 113-143, 2006.
Redfern, S.A.T., Neutron powder diffraction studies of order-disorder phase transitions and kinetics, in Neutron Scattering in Earth Sciences, pp. 145-170, 2006.

## Mineral Physics and Chemistry

Alvarez, M., E.H. Rueda, and E.E. Sileo, Simultaneous incorporation of Mn and Al in the goethite structure, Geochimica Et Cosmochimica Acta, 71 (4), 1009-1020, 2007.
Aquino, A.J.A., D. Tunega, G. Haberhauer, M.H. Gerzabek, and H. Lischka, Quantum chemical adsorption studies on the (110) surface of the mineral goethite, Journal of Physical Chemistry C, 111 (2), 877-885, 2007.
Burkhard, D.J.M., and H. Muller-Sigmund, Surface alteration of basalt due to cation-migration, Bulletin of Volcanology, 69 (3), 319-328, 2007.
Busigny, V., and N. Dauphas, Tracing paleofluid circulations using iron isotopes: A study of hematite and goethite concretions from the Navajo Sandstone (Utah, USA), Earth and Planetary Science Letters, 254 (3-4), 272-287, 2007.
Djordjevic, M., and M. Munzenberg, Connecting the timescales in picosecond remagnetization experiments, Physical Review B, 75 (1), 2007.
Elzinga, E.J., and D.L. Sparks, Phosphate adsorption onto hematite: An in situ ATR-FTIR investigation of the effects of pH and loading level on the mode of phosphate surface complexation, Journal of Colloid and Interface Science, 308 (1), 53-70, 2007.
Hou, D.L., Z.X. Du, C.X. Yue, and Q.H. Liu, Studies on magnetic aftereffect of Fe3O4 nano-particles, Journal of Alloys and Compounds, 429 (1-2), 40-45, 2007.
Letard, I., P. Sainctavit, and C. Deudon, XMCD at Fe L-2,L-3 edges, fe and SK edges on Fe7S8, Physics and Chemistry of Minerals, 34 (2), 113-120, 2007.
Majzlan, J., L. Mazeina, and A. Navrotsky, Enthalpy of water adsorption and surface enthalpy of lepidocrocite (gamma-FeOOH), Geochimica Et Cosmochimica Acta, 71 (3), 615-623, 2007.
Mazeina, L., and A. Navrotsky, Enthalpy of water adsorption and surface enthalpy of goethite (alpha-FeOOH) and hematite (alpha-Fe2O3), Chemistry of Materials, 19 (4), 825-833, 2007.
Paananen, T., Effect of impurity element on reduction behaviour of magnetite, Steel Research International, 78 (2), 91-95, 2007.
Pasternak, M.P., and R.D. Taylor, Mossbauer spectroscopy methodology at the cutting-edge of high-pressure research, Hyperfine Interactions, 170 (1-3), 15-32, 2006.
Rozenberg, G.K., Y. Amiel, W.M. Xu, M.P. Pasternak, R. Jeanloz, M. Hanfland, and R.D. Taylor, Structural characterization of temperature- and pressure-induced inverse <-> normal spinel transformation in magnetite, Physical Review B, 75 (2), 2007.
Tabor, N.J., Permo-Pennsylvanian palaeotemperatures from Fe-Oxide and phyllosilicate delta O-18 values, Earth and Planetary Science Letters, 253 (1-2), 159-171, 2007.
Yapp, C.J., Oxygen isotopes in synthetic goethite and a model for the apparent pH dependence of goethite-water O-18/O-16 fractionation, Geochimica Et Cosmochimica Acta, 71 (5), 1115-1129, 2007.

## Nanophase and Disordered Systems

Fernandez-Rossier, J., and R. Aguado, Single-electron transport in electrically tunable nanomagnets, Physical Review Letters, 98 (10), 2007.
Halim, K.S.A., M.H. Khedr, M.I. Nasr, and A.M. El-Mansy, Factors affecting CO oxidation over nanosized Fe2O3, Materials Research Bulletin, 42 (4), 731-741, 2007.
Kruglyak, V.V., P.S. Keatley, R.J. Hicken, J.R. Childress, and J.A. Katine, Dynamic configurational anisotropy in nanomagnets, Physical Review B, 75 (2), 2007.
Wang, S.B., Y.L. Min, and S.H. Yu, Synthesis and magnetic properties of uniform hematite nanocubes, Journal of Physical Chemistry C, 111 (9), 3551-3554, 2007.
Zhao, Y.M., C.W. Dunnill, Y.Q. Zhu, D.H. Gregory, W. Kockenberger, Y.H. Li, W.B. Hu, I. Ahmad, and D.G. McCartney, Low-temperature magnetic properties of hematite nanorods, Chemistry of Materials, 19 (4), 916-921, 2007.

## Synthesis

Dou, J., L. Navarrete, P. Kale, P. Padmini, R.K. Pandey, H. Guo, A. Gupta, and R. Schad, Preparation and characterization of epitaxial ilmenite-hematite films, Journal of Applied Physics, 101 (5), 2007.

## Paleomagnetism and Tectonics

Awschalom, D.D., and M.E. Flatte, Challenges for semiconductor spintronics, Nature Physics, 3 (3), 153-159, 2007.
Hankard, F., J.P. Cogne, V.A. Kravchinsky, L. Carporzen, A. Bayasgalan, and P. Lkhagvadorj, New Tertiary paleomagnetic poles from Mongolia and Siberia at 40, 30, 20, and 13

The IRM Quarterly

The *Institute for Rock Magnetism* is dedicated to providing state-of-the-art facilities and technical expertise free of charge to any interested researcher who applies and is accepted as a Visiting Fellow. Short proposals are accepted semi-annually in spring and fall for work to be done in a 10-day period during the following half year. Shorter, less formal visits are arranged on an individual basis through the Facilities Manager.

The *IRM* staff consists of **Subir Banerjee**, Professor/Director; **Bruce Moskowitz**, Professor/Associate Director; **Jim Marvin**, Emeritus Scientist; **Mike Jackson**, **Peat Sølheid**, and **Brian Carter-Stiglitz**, Staff Scientists.

Funding for the *IRM* is provided by the **National Science Foundation**, the **W. M. Keck Foundation**, and the **University of Minnesota**.

The *IRM Quarterly* is published four times a year by the staff of the *IRM*. If you or someone you know would like to be on our mailing list, if you have something you would like to contribute (*e.g.*, titles plus abstracts of papers in press), or if you have any suggestions to improve the newsletter, please notify the editor:

**Brian Carter-Stiglitz**
Institute for Rock Magnetism
University of Minnesota
289 Shepherd Laboratories
100 Union Street S. E.
Minneapolis, MN 55455-0128
phone: (612) 624-5049
fax: (612) 625-7502
e-mail: cart0196@umn.edu
www.irm.umn.edu




UNIVERSITY OF MINNESOTA

Ma: Clues on the inclination shallowing problem in central Asia, Journal of Geophysical Research-Solid Earth, 112 (B2), 2007.

Piper, J.D.A., Palaeomagnetism of the Loch Doon Granite Complex, Southern Uplands of Scotland: The Late Caledonian palaeomagnetic record and an Early Devonian episode of True Polar Wander, Tectonophysics, 432 (1-4), 133-157, 2007.

Somoza, R., Eocene paleomagnetic pole for South America: Northward continental motion in the Cenozoic, opening of Drake Passage and Caribbean convergence, Journal of Geophysical Research-Solid Earth, 112 (B3), 2007.

Strik, G., M.J. de Wit, and C.G. Langereis, Palaeomagnetism of the Neoarchaean Pongola and Ventersdorp Supergroups and an appraisal of the 3.0-1.9 Ga apparent polar wander path of the Kaapvaal Craton, Southern Africa, Precambrian Research, 153 (1-2), 96-115, 2007.

Tan, X.D., K.P. Kodama, S. Gilder, and V. Courtillot, Rock magnetic evidence for inclination shallowing in the Passaic Formation red beds from the Newark basin and a systematic bias of the Late Triassic apparent polar wander path for North America, Earth and Planetary Science Letters, 254 (3-4), 345-357, 2007.

University of Minnesota
291 Shepherd Laboratories
100 Union Street S. E.
Minneapolis, MN 55455-0128
phone: (612) 624-5274
fax: (612) 625-7502
e-mail: irm@umn.edu
www.irm.umn.edu